

Analysis and Optimization of Wireless Power Transfer Link

Ajay Kumar Sah, Dibakar Raj Pant

Department of Electronics and Computer Engineering, Central Campus, Pulchowk, IOE, Tribhuvan University, Nepal

Corresponding Email: ajayshah2005@yahoo.com pdibakar@gmail.com

Abstract: In this paper, a high efficiency Gallium nitride (GaN), HEMT (High Electron Mobility Transistor) class-E power amplifier for the wireless power transfer link is designed and simulated on PSpice. A four-coil wireless power transfer link is modeled for maximum power transfer efficiency on ADS (Advanced Design System) and frequency splitting phenomenon is demonstrated, explained and analyzed. Two resonant coupling structures, series & mixed, are presented and compared. The efficiency performance of the link is studied using spiral and helical antennas of different wire make. In addition, techniques for improving efficiency of the wireless power transfer systems with changing coupling coefficient viz. frequency splitting phenomenon of the coils are proposed.

Keywords: Wireless Power Transfer, Resonant coupling, Frequency Splitting, GaN HEMT, Power transfer efficiency.

1. Introduction

In recent days, research on wireless power transmission has been increasing due to many benefits in Electronics and Communication engineering. The examples are: wireless charging of implantable medical devices like ventricular assist devices, pacemaker, etc. and consumer electronics such as phones, laptops, and etc. [1]. The history of wireless power transmission dates back to the late 19th century with the prediction that power could be transmitted from one point to another in free space by Maxwell in his “Treatise on Electricity and Magnetism”. Heinrich Rudolf Hertz performed experimental validation of Maxwell’s equation which was a monumental step in the direction. However, Nikola Tesla’s experiments are often considered as being some of the most serious demonstrations of the capability of transferring power wirelessly even with his failed attempts to send power to space [2].

Recently, MIT proposed a new scheme based on strongly coupled magnetic resonances, thus presenting a potential breakthrough for a mid-range wireless energy transfer. The fundamental principle is that resonant objects exchange energy efficiently, while non-resonant objects do not. The scheme is carried with a power transfer of 60 W and has RF-to-RF coupling efficiency of 40% for a distance of 2 m, which is more than three times the coil diameter. We expect that coupled magnetic resonances will make possible the commercialization of a midrange wireless power transfer [3]. Inductive coupling has been the most popular method for wireless power transfer, which requires two coils (primary and secondary coils). The efficiency of power transfer between the coils is a strong function of the coil dimensions and distance between them, which is an undesired trend in the case of freely-moving subjects. Therefore, the recent

alternative method of resonance-based power delivery has been suggested by [3] in 2007 and is explained through the coupled-mode theory [4]. This multiple-coil based approach is used to decouple adverse effects of source and load resistance from the coils, and in this way achieve a high quality factor for them. This method is less sensitive to changes in the coil distance and typically employs two pairs of coils: one in the external circuit called driver and primary coils, and the other in the receiver side called secondary and load coils.

Although magnetic resonance has significant advantage in transmission distance compared with electromagnetic induction, this technology has intrinsic limitation as the load absorption power is sensitive to variations in the operating parameters, and small differences in operating and resonance frequency will reduce transmission performance significantly moreover when the coupling coefficient changes, there is the frequency splitting issue which substantially reduces the system efficiency.

In this paper, a high efficiency Gallium nitride (GaN), HEMT (High Electron Mobility Transistor) class-E power amplifier for the wireless power transfer link is designed and simulated on PSpice. A four-coil wireless power transfer link is modeled for maximum power transfer efficiency on ADS (Advanced Design System) and frequency splitting phenomenon is demonstrated, explained and analyzed.

2. Related Theory

A. Inductance

The inductance of circular/helical structure can be computed as follows [8]:

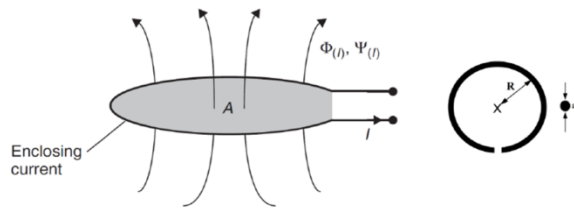


Figure 1: Inductance Definition

$$L = N^2 \mu R \left[\ln \left(\frac{8R}{a} \right) - 2 \right] \quad 1$$

Where:

N: Number of turns

μ : Relative permeability

R: Radius of the coil

a: Radius of the cross section of the coil

Inductance is one of the characteristic variables of conductor coils. The inductance of a conductor coil depends totally upon the material properties (permeability) of the space that the flux flows through and the geometry of the layout.

B. Mutual Inductance

Closed form equations for the mutual inductance of two filamentary coils for all physical arrangements have been derived [8-9]. Figure 2 shows all relevant variables for calculations.

The relevant equations defining the mutual inductance between two such coils are as follows:

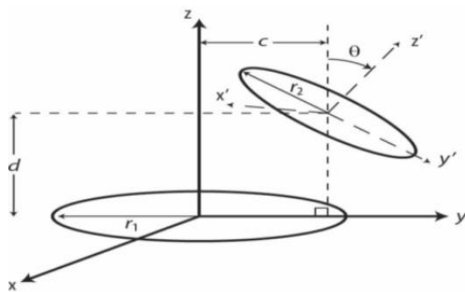


Figure 2: Two coils with variable defined for all positions.

The relevant equations defining the mutual inductance between two such coils are as follows [10]:

$$M_{12} = \frac{2\mu_0}{\pi} \sqrt{r_1 r_2} \int_0^\pi \frac{\left[\cos\theta - \frac{c}{r_2} \cos\phi \right]}{k \sqrt{V^2}} \varphi(k) d\phi \quad 2$$

Where,

$$\alpha = \frac{r_2}{r_1} \quad \text{and} \quad \beta = \frac{d}{r_1}$$

$$V = \sqrt{\left(1 - \cos^2\phi \sin^2\theta - 2 \frac{c}{r_2} \cos\phi \cos\theta + \frac{c^2}{r_2^2}\right)}$$

$$k^2 = \frac{4\alpha V}{(1 + \alpha V)^2 + \zeta^2} \quad \text{and} \quad \zeta = \beta - \alpha \cos\phi \sin\theta$$

$$\varphi(k) = \left(1 - \frac{k^2}{2}\right) K(k) - E(k)$$

Where $K(k)$ and $E(k)$ are complete elliptic integrals of the first and second kind, respectively, as follows:

$$K(k) = \int_0^{\frac{\pi}{2}} \frac{d\beta}{\sqrt{1 - k^2 \sin^2\beta}}$$

$$E(k) = \int_0^{\frac{\pi}{2}} \sqrt{1 - k^2 \sin^2\beta} d\beta$$

These equations define the mutual inductance between two coils for any configurations.

Simplified Mutual Inductance for Co-Axial Coils:

The mutual inductance for two coils aligned co-axially (along the same central axis) as shown in Figure 2 reduce to a less complex equation.

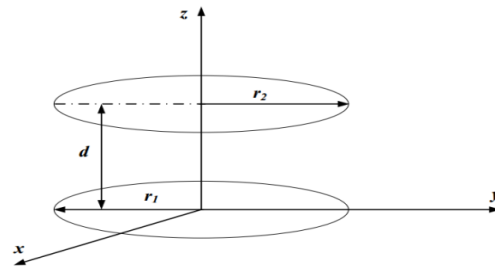


Figure 3: Two coils aligned co-axially

The mutual inductance was solved by application of Neumann's relations in [8]. Equation (2) reduces to:

$$M_{12} = \mu \sqrt{r_1 r_2} \left[\left(\frac{2}{k} - k \right) K - \frac{2}{k} E \right] \quad 3$$

Where,

$$k^2 = \frac{4 r_1 r_2}{(r_1 + r_2)^2 + d^2}$$

C. Coupling Coefficient

Generally, the amount of inductive coupling that exists between the two coils is expressed as a fractional number between 0 and 1 instead of a percentage value, where 0 indicates zero or no inductive coupling, and 1 indicates full or maximum inductive coupling. In other words, if k is equal to 1, the two coils are perfectly coupled, if k is greater than 0.5 the two coils are said to be tightly coupled and if k is less than 0.5, the two coils

are said to be loosely coupled. Then the equation of mutual inductance which assumes a perfect coupling can be modified to take into account this coefficient of coupling, k and is given as

$$k = \frac{M}{\sqrt{L_1 L_2}} \quad 4$$

When the coefficient of coupling, k is equal to 1, such that all the lines of flux of one coil cut all of the turns of the other, the mutual inductance is equal to the geometric mean of the two individual inductances of the coils. So, when the two inductances are equal and L1 is equal to L2, the mutual inductance that exists between the two coils can be defined as

$$M = \sqrt{L_1 L_2} = L \quad 5$$

D. Coil Antenna

A single-layer coil has two advantages. Firstly, like all air core coils, it is free from 'iron losses' and the non-linearity. Secondly, single-layer coils have the additional advantage of low self-capacitance and thus high self-resonant frequency. These coils are mostly used above about 3 MHz.

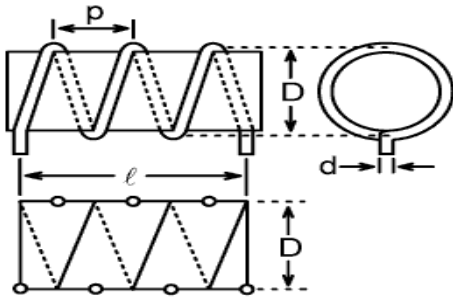


Figure 4: Single Layer Coil

For a single-layer solenoid coil the inductance may be estimated as follows [9]:

$$L = 4\pi 10^4 N^2 R L \left[\log_{10}(1 + \pi F) + \left\{ \frac{1}{2.3 + \frac{1.6}{F} + \frac{0.44}{F^2}} \right\} \right] 6$$

Where,

N = number of turns

R = coil radius in mm

F = ratio (coil radius/coil length)

L = μH

The inductance of a multi-layer air cored coil is given by [8]:

$$L = XN^2(D + A) \quad 7$$

Where

$$X = \frac{\pi^2(\alpha + 1.3r + 0.1)}{(20\alpha + 30r + 10)(100\alpha + 107r + 7)} \log_{10} \left[100 + \frac{7(1+r)}{2\alpha + 3r} \right]$$

$$\alpha = \frac{C}{D + A}$$

$$r = \frac{A}{D + A}$$

and,

D = core diameter (cm)

C = core length (cm)

A = coil depth (cm)

L = μH

E. Inductor Wire

There are mainly two types of wires, solid wires and stranded wires. Solid wire is composed of a single piece of metal wire, also known as a strand. Stranded wire is composed of many pieces of solid wire all bundled into one group.

American wire gauge (AWG), also known as the Brown & Sharpe wire gauge, is a standardized wire gauge system used since 1857 predominantly in North America for the diameters of round, solid, nonferrous, electrically conducting wire. The AWG table given below is for a single, solid, round conductor from 10 to 22 AWG with cross sectional area, diameter and resistance [12].

Table 1: American wire gauge chart

AWG Number	\varnothing [Inch] for Solid Rod	\varnothing [mm] for Solid Rod	\varnothing [mm ²] for Solid Rod	Resistance [Ohm/m] Copper (20 °C, 68 °F)
10	0.102	2.59	5.26	0.00328
12	0.0808	2.05	3.31	0.00521
14	0.0641	1.63	2.08	0.00829
16	0.0508	1.29	1.31	0.0132
18	0.0403	1.02	0.823	0.0210
20	0.0320	0.812	0.518	0.0333
22	0.0253	0.644	0.326	0.0530

F. Class-E Amplifier

The class-E is a switch mode amplifier designed for very high power efficiency. It is nonlinear in the sense that the output amplitude does not correspond to the input amplitude. In order to adjust the output amplitude the supply voltage can be adjusted. It is primarily made for high frequency applications and is commonly used to create carrier waves for radio transmissions. Figure 5 shows an ideal E-class circuit.

It consists of an RF choke L_c , a switch T_1 , a shunt capacitor (which includes the transistor capacitance) C_s , a load networks L-C and a load R_L . The switch is operated at the desired output frequency, for maximum efficiency a 50% duty cycle is used.

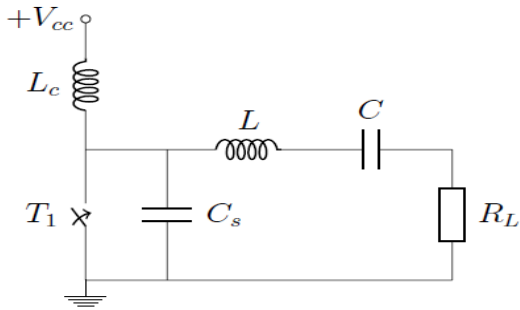


Figure 5: Class-E amplifier

The load network gives the required phase shift to prevent high current and high voltage at the switch, transistor, and acts as an open circuit for the first harmonic, passing a sine wave to the load. There are some conditions that should be fulfilled in order to make it as efficient as possible, when the switch goes from open to closed, the voltage over the switch, V_{T1} is supposed to behave as

$$V_{T1} = 0 \quad 8$$

$$\frac{dV_{T1}}{dt} = 0 \quad 9$$

To fulfill these conditions the following expressions have been derived [16]. The power delivered to the load is given by

$$R_L = \frac{(V_{cc} - V_o)^2}{P} 0.576801 \left(1.001245 + \frac{0.451759}{Q_L} - \frac{0.402444}{Q_L^2} \right)$$

Where V_{cc} is the supply voltage, V_o the transistor saturation voltage (0 for FET transistors), R_L is the load, and Q_L is the loaded quality factor. The shunt capacitor is then given by

$$C_s = \frac{1}{2\pi f R_L \left(\frac{\pi^2}{4} + 1 \right) \frac{\pi}{2}} \left(0.998666 + \frac{0.91424}{Q_L} - \frac{1.03175}{Q_L^2} \right) + \frac{0.6}{(2\pi f)^2 L_c}$$

Where L_c is the choke inductor and the load network

$$C = \frac{1}{2\pi f R_L \left(\frac{1}{Q_L - 0.104823} \right)} \left(1.00121 + \frac{1.01468}{Q_L - 1.7879} \right) - \frac{0.2}{(2\pi f)^2 L_c}$$

and,

$$L = \frac{Q_L R_c}{2\pi f}$$

The design choices left to do is to specify the supply voltage V_{cc} , the output power P and the quality factor Q_L .

G. GaN HEMT

GaN HEMT is a High Electron Mobility Transistor (HEMT). It is a binary III/V direct band gap semiconductor commonly used in bright light-emitting diodes since the 1990s. The compound is a very hard material. Its wide band gap of 3.4 eV affords it special properties for applications in optoelectronic, high-power and high-frequency devices. For example, GaN is the substrate which makes violet (405 nm) laser diodes possible, without use of nonlinear optical frequency-doubling. Because GaN transistors can operate at much higher temperatures and work at much higher voltages than gallium arsenide (GaAs) transistors, they make ideal power amplifiers at microwave frequencies [17].

Enhancement mode Gallium Nitride (GaN) power FETs can provide significant power density benefits over silicon MOSFETs in power converters. They have a much lower figure of merit (FOM) due to lower R_{dson} and lower Q_g . With greater efficiencies, faster switching frequencies, and an ultra-small package footprint, GaN FETs enable higher density power converters. However, realizing these benefits does present a new set of challenges. Large source-drain voltages and the stringent gate-source voltage drive requirements of GaN power FETs pose new challenges related to limiting the high-side FET drive level to less than 6V, as well as preventing high dV/dt transients from causing erratic switching behavior [18].

Due to high mobility of carrier electron, HEMT has very low stray capacitance such as C_{gs} and C_{ds} . Low C_{gs} enables high frequency gate drive with low input power. Low C_{ds} enables low switching loss for switched power supplies. For class-E amplifiers, low C_{ds} enables capability of high operating frequency because the shunt capacitance of class-E amplifier includes output capacitance of transistor, i.e., C_{ds} . And, lowest limit of shunt capacitance, i.e., C_{ds} determines the highest limit of operating frequency. Further, high breakdown voltage extends capability of applying class-E amplifier for high frequency and high power applications. This is because peak switch voltage of class-E amplifier is 3.56 times higher than dc supply voltage when the amplifier is operating at nominal condition and duty ratio 0.5[18].

3. WPT System Design Calculations

A. Block Diagram of 4 coil WPT System

The block diagram of the 4 coil WPT system is shown in figure 6 below. Major blocks in a WPT system include the power amplifier, the transmitting and receiving coils, and the receiver.

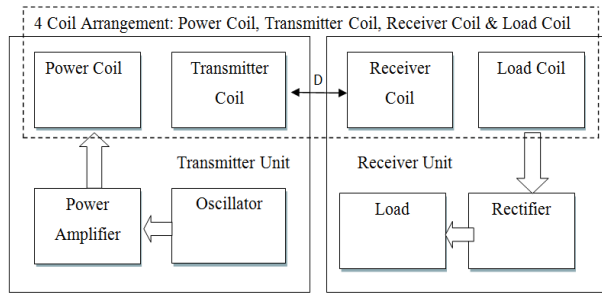


Figure 6: Block diagram of 4 coil WPT system

The oscillator receives supply voltage through rectifier from ac source which is not shown in the figure. The oscillator produces signal of required frequency and then gets amplified by power amplifier. The amplified signal is given to the power coil. When the transmitting antenna begins to resonate, it generates the evanescent resonate waves and receiver coil will pick these waves up.

Within the system, the power amplifier is one of the most important components because it determines the performance of the system, acting not only as the power converter, but also as the control mechanism. Therefore, this work proposes a high efficiency GaN class-E power amplifier for the WPT application to obtain an excellent characteristic.

Design of GaN HEMT Class-E Power Amplifier:

Setting V_{cc} to 5V, R_L to 1 Ohm, L_c to 100uH and Q_L to 10 and using equations from section F, gives the component values displayed in Table 2. The switch is replaced by GaN HEMT enhancement type MOSFET transistor, EPC1010, which has a low R_{dson} and small gate charge in order to be efficient and easy to drive [19]. Instead of gate driver, VPULSE input is used to drive the transistor, to make it as close to an ideal switch as possible. All the components used are shown in Table 2.

Table 2: Deign Limits

Transistor	EPC1010
Gate Driver	PSPICE VPULSE
C	0.9735nF
Cs	1.6967nF
L	0.1608uH
Load Resistance	1.37 Ohm

With all components selected, the class-E amplifier is implemented in PSpice. In PSpice the transient behavior of the circuit is studied. It can be seen that the voltage and the current behave similar to Eq. 8 and 9 and that the output is a nice sine wave.

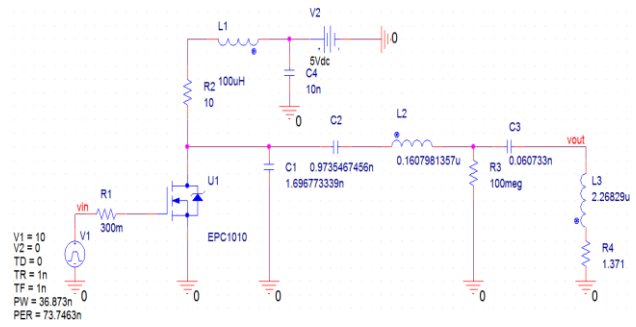


Figure 7: GaN class-E amplifier PSpice Schematic

The load R_L is replaced by a series RLC circuit, representing the transmitting coil and capacitance. The resistor is the coil resistance and at the resonance frequency the inductor and capacitor will cancel out leaving only the resistance. The 100M resistor is only added to make simulations possible and will not affect the circuit. Figure 7 shows the schematic of the complete and tuned circuit. The transistor dc voltage along with the output voltage is shown in figure 8.

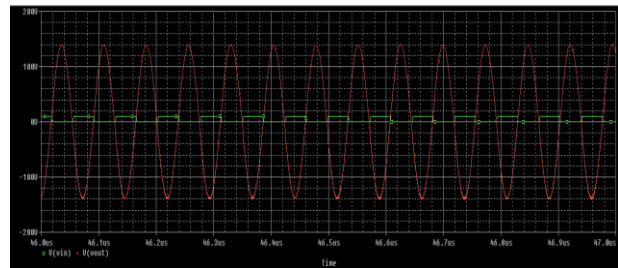


Figure 8: Transient analysis of GaN class-E amplifier

It can be seen from the figure 8, the input to the class-E amplifier is 5v square wave and the output is 160v sine wave.

B. Parameter Identification of Proposed System

We have from (20),

$$L = \frac{N^2 R^2}{2.54(9R + 10H)}$$

Where,

L = inductance in micro-Henries

N = number of turns of wire

R = radius of coil in cm

H = height of coil in cm

The quality factor is presented in a formula as given below

$$Q_i = \frac{1}{R_i} \sqrt{\frac{L_i}{C_i}} = \frac{\omega_i L_i}{R_i} \Leftrightarrow \omega_i L_i = R_i Q_i, i = 1 \sim 4 \quad 10$$

Where, ω_i and R_i are respectively the self-resonant frequency and equivalent resistance of each resonant circuit. In the power coil, for instance, R_i is a sum of R_S and R_1 .

The Coupling Coefficient between Transmitter & Receiver is given by

$$k_{23}^* = \sqrt{\frac{(1 + k_{12}^2 Q_1 Q_2)(1 + k_{34}^2 Q_3 Q_4)}{Q_2 Q_3}} \quad 11$$

And the maximum value of magnitude of S_{21} parameter is given as follows

$$|S_{21}|_{\max} = \frac{k_{12} k_{34} Q_1 Q_4 R_L}{k_{23}^* \sqrt{L_1 L_4} \omega_0} \quad 12$$

Power Transfer Efficiency of the WPT system is calculated by,

$$\eta_{21} = S_{21}^2 \times 100 \% \quad 13$$

The equivalent circuit of whole WPT system is modeled as RLC electrical circuit. The parameters used are from table which is taken from [20].

The design parameters for all the antenna is listed in the table below:

Table 3: Parameters of designed antenna

Coil (antenna)	N (turns)	R (cm)	H (cm)	L (uH)	F (MHZ)	C (Pf)
Power	2	5	3.3	0.5	13.56	275.518
Transmitter	3	6	4.4	1.3	13.56	105.968
Receiver	1.67	6	4.4	0.4	13.56	344.398
Load	1	3.7	2	0.1	13.56	1.377nf

From equation (11) and (12), with the value given in Table 3, quality factors, coupling coefficient and the maximum value of magnitude of S_{21} parameter is calculated. The values are as follows

$$\omega_0 = \omega_1 = \frac{1}{\sqrt{L_1 C_1}} \approx 85.2 \times 10^6 [\text{rad/s}]$$

From equation (4.4), assuming $R_S=R_L=50$ Ohm and $R_1=R_2=R_3=R_4=0.015$ Ohm,

$$Q_1 \approx 1.7, Q_2 = 7384, Q_3 = 2272, Q_4 \approx 0.17$$

The coupling coefficient is calculated as,

$$k_{23}^* = 4.29 \times 10^{-3}$$

The maximum value of magnitude of S_{21} parameter is calculated as follows

$$|S_{21}|_{\max} \approx 0.884$$

Power Transfer Efficiency of the WPT system is calculated as,

$$\eta_{21} = S_{21}^2 \times 100 \% = 78.2\%$$

4. Frequency Splitting and Cause Analysis

The equivalent circuit model of whole WPT system is simulated by using an advanced design system (ADS), a popular electric automation tool in RF engineering of Agilent Technologies with the circuit setup illustrated in Figure 9.

The equivalent circuit model to calculate the maximum power transfer efficiency ($\eta_{21} = S_{21}^2 \times 100 \%$) is shown in Figure 10.

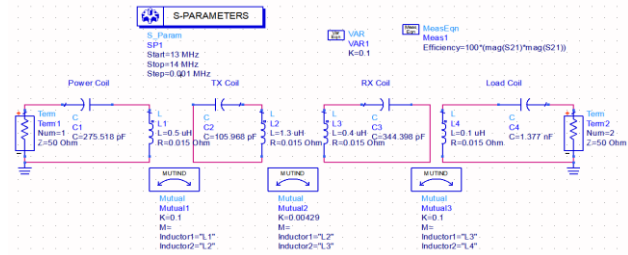


Figure 9: Simulation set up for Power transfer efficiency

The result of power transfer efficiency of the designed WPT system is shown in Figure 10.

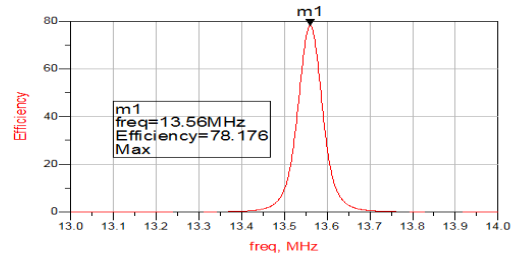


Figure 10: Power transfer efficiency of WPT system

The maximum power transfer efficiency of the WPT system as seen from the above result is equal to 78.176% which is very close to the theoretically calculated maximum power transfer efficiency 77.79%. The above results can be tabulated as shown in Table 4.

Table 4: Theoretical and Simulated Efficiency of WPT System

Parameter	Theoretical	Simulation
Maximum Power Transfer	0.884	0.884
Power transfer efficiency	78.2%	78.18%

The value of magnitude of S_{21} of designed WPT System for three different coupling coefficients which is a function of distance between transmitter and receiver is shown in Figure 11. The coupling coefficient decreases as the distance increases or vice versa.

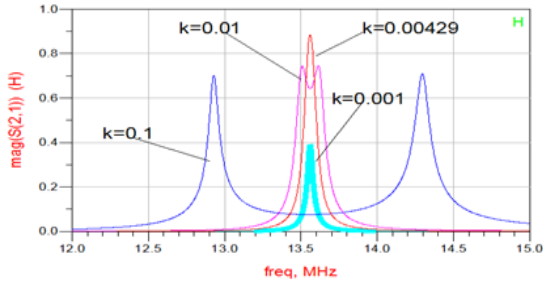


Figure 11: Simulation result showing $|S_{21}|$ at different k_{23}

Figure 11 reveals how efficiency varies with frequency at different distances. At remote distances, the efficiency peaks only at the resonant frequency. Closer distance leads to frequency splitting. The efficiency peaks at both below and above the original resonant frequency. The shorter the transfer distance, more obvious the phenomena is.

Efficiency reflects the distribution of the input power in the viewpoint of power flow. The input power is consumed in three aspects, i.e. the loss of the source internal resistance, the ohmic losses of the resonant coils, and the load. High efficiency is achieved when the bulk of the input power is consumed in the load. Any increase in the share of the ohmic losses of the source internal resistance and the resonant coils leads to lowered efficiency. As a consequence, analyzing the effects of the source internal resistance and the equivalent resistances of the resonant coils is of great importance to frequency splitting. The expression of the input impedance is deduced to examine how the input impedance responds to the distance (namely M_{23}). At the resonant frequency, the input impedance can be expressed as [21-24]:

$$Z_{in} = j\omega L_1 + \frac{(\omega M_{12})^2}{R_2 + j\omega L_2 + \frac{1}{j\omega C_2} + \frac{(\omega M_{23})^2}{R_3 + j\omega L_3 + \frac{1}{j\omega C_3} + j\omega L_4 + Z_L}} \quad 14$$

$$= j\omega L_1 + \frac{(\omega M_{12})^2}{R_2 + \frac{(\omega M_{23})^2}{R_3 + \frac{(\omega M_{34})^2}{j\omega L_4 + Z_L}}}$$

Owing to the fact that the reduced distance leads to the dramatic increase of the mutual inductance M_{23} , the amplitude of the input impedance is declining and the angle is reaching towards 90° , close to pure inductiveness. At close distances, the input impedance is characteristic of large impedance angle and low amplitude. The real part of the input impedance is proportional to the power transferred and consumed from the source to the source loop, and the imaginary part is in proportion to the power exchanged between the source and the source loop. On the one hand, the

amplitude of the input impedance at close distances is small enough to produce a large current in the source loop, thus leading to a large source internal resistance loss. On the other hand, due to the extremely large impedance angle, the transferred power only accounts for a small proportion of the large input power in the source loop. Much power is exchanged between the source and the source loop, without being transferred to the load. Therefore, efficiency drops sharply.

In conclusion, the explanation for frequency splitting is provided as follows. Close distances lead to the great influence of the source internal resistance on efficiency. At close distances, the input impedance at the original resonant frequency point is characteristic of extremely large impedance angle and relatively low amplitude. Large impedance angle causes very low transferred power, and much is exchanged between the source and the source loop. Small amplitude results in a large source current, thus increasing the source internal resistance loss. Both of these two factors reduce efficiency. While at below and above the original resonant frequency, the input impedance is characteristic of extremely small impedance angle and relatively high amplitude. Due to the opposite characteristics, efficiency peaks at these two frequency points.

Frequency splitting occurs when the input impedance is changed into small amplitude and large impedance angle at close distances. In this section, the related factors, i.e. the source internal resistance (R_s), the mutual inductance between the Power coil and the Transmitter coil (M_{12}), and the mutual inductance between the load loop and the receiving loop (M_{34})[24], will be explored to pursue investigation into their impacts on frequency splitting.

A. Source Internal Resistance

On the basis of the analysis above, it can be expected that an increase of the source internal resistance will highlight the frequency splitting phenomena. Moreover, with a large enough increase in the source internal resistance, frequency splitting will also appear on the occasions where frequency splitting does not occur previously.

B. Mutual Inductance of Source & Transmitter Coil

The mutual inductance of the Power coil and the Transmitter coil (M_{12}) affects the amount of power transferred from the Power coil to the Transmitter coil. For a given current in the power coil, the larger the mutual inductance M_{12} , the larger the induced current in the Transmitter coil. Once the transferred power

accounts for a significant proportion, frequency splitting will be greatly reduced or completely absent.

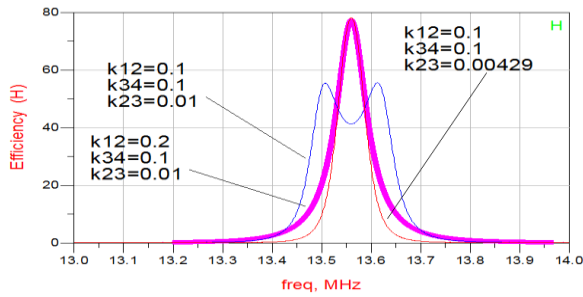


Figure 12: Power transfer efficiency at different coupling coefficient

It can be seen from the figure 12 that decreasing the coupling coefficient k_{23} between transmitter & receiver coil i.e. bringing the transmitter and receiver closer keeping the k_{12} & k_{34} fixed, efficiency of the system decreases and frequency splitting takes place. When the coupling between power coil and transmitter coil k_{12} increase from 0.1 to 0.2 i.e. bringing the power coil and transmitter coil closer eliminates the frequency splitting phenomena and the efficiency of the system increases.

C. Mutual Inductance of Load & Receiver Coil

Similar to M_{12} , the mutual inductance of the load and the receiver coil (M_{34}) influences the power transferred from the receiver coil to the load coil. For a given current in the receiver coil, the larger the mutual inductance M_{34} , the larger the induced current in the load coil. Once the transferred power to the load accounts for a significant proportion, frequency splitting will be reduced.

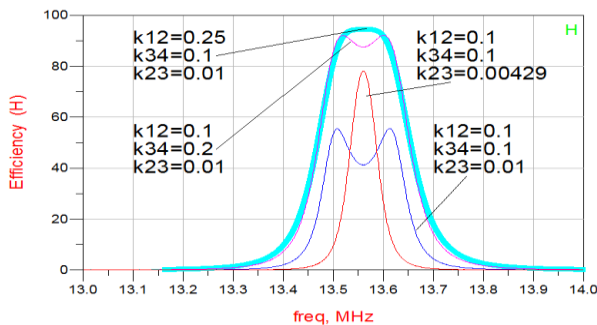


Figure 13: Power transfer efficiency at different coupling coefficient

It can be seen from the figure 13 that decreasing the coupling coefficient k_{23} between transmitter & receiver coil i.e. bringing the transmitter and receiver closer keeping the k_{12} & k_{34} fixed, efficiency of the

system decreases and frequency splitting takes place. When the coupling between receiver coil and load coil k_{34} increases from 0.1 to 0.25 i.e. bringing the receiver coil and load coil closer eliminates the frequency splitting phenomena and the efficiency of the system increases.

Based on the power flow, the cause for frequency splitting is revealed. The source internal resistance plays a dominant role in efficiency at close distances. The characteristics of the input impedance at close distances at the original resonant frequency, namely extremely high impedance angle and relatively small amplitude, lead to decreasing efficiency. While at both above and below the original resonant frequency, two efficiency peaks arise due to the low impedance angle and relatively high amplitude of the input impedance. Related factors of the frequency splitting phenomena, namely the source internal resistance, the mutual inductance of the Power coil and the Transmitter coil, and the mutual inductance of the load loop and the receiving loop, are studied through theoretical calculations and simulations. It is found that reducing the source internal resistance, and increasing the mutual inductance of the Power coil and the Transmitter coil, as well as the mutual inductance of the load loop and the receiving loop, all help relieve the frequency splitting phenomena and improve efficiency.

5. Comparative Study on Antenna Topology

Most of the wireless power transfer system to this time has been designed using series-series topology of antenna system. The researchers are focused on various factors like coil size, coil material, operating frequency but not on antenna topology to improve efficiency. Here using the same parameters as used in series-series topology, a mixed topology called LCC topology is analyzed.

The resonant frequency of LCC circuit, neglecting internal resistance of the coil is calculated as [13]:

$$f = \frac{1}{2\pi\sqrt{L(C_1 + C_2)}} \quad 15$$

Where,

L = Parallel Inductance, C_1 = Series Capacitance, C_2 = Parallel Capacitance

Using Wheeler formula and following similar procedure as in section III, the design parameters for all the antenna is listed in the table below:

Table 5: Design parameters for all the antenna

Coil (antenna)	N (turns)	R (cm)	H (cm)	L (uH)	F (MHZ)	C1 (Pf)	C2 (Pf)
Power	2	5	3.3	0.5	13.56	150	125.52
Transmitter	3	6	4.4	1.3	13.56	75	30.97
Receiver	1.67	6	4.4	0.4	13.56	125	219.4
Load	1	3.7	2	0.1	13.56	300	1077.6

The LCC equivalent circuit model of whole WPT system is simulated on advanced design system (ADS), a popular electric automation tool in RF engineering of Agilent Technologies with the circuit setup illustrated in Figure 14.

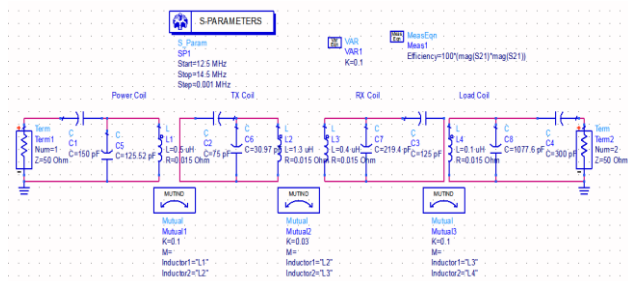


Figure 14: Simulation set up for Power transfer efficiency for LCC topology

The parameters' values are taken from the table 5. The radius of power coil is 5 cm, the radius of load coil is 3.7 cm, radius of transmitter and receiver coil is 6cm. The power coil has two turns, load coil has one turn, transmitter coil has three turns and receiver coil has 1.67 turns.

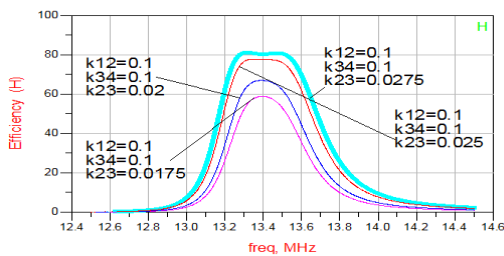


Figure 15: Power transfer efficiency at different k for LCC

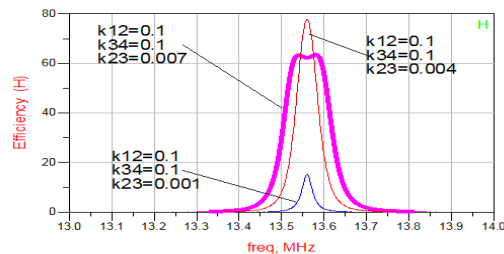


Figure 16: Power transfer efficiency at different k for series-series topology

The result of power transfer efficiency of the LCC WPT system is shown in figure 15. The result of power transfer efficiency of the series-series WPT system is shown in figure 16.

6. Comparative Study on Different Gauge Wire

Inductor coils or coil antennas are made by wires. The wires are solid and strand types. Different wires are different in properties. They have different electrical properties. The skin depth is defined as:

$$\delta = \sqrt{\frac{2}{\omega\sigma\mu}}$$

With $\sigma=5.96 \times 10^7$ for copper. For $f=13.56$ MHz, the skin depth is $\approx 18\mu m$.

According to the skin depth at 13.56 MHz, American Gauge Wire 10 to 22 can be used for the wireless power transfer antenna system at this frequency but for the study purpose only AWG14, 18 and 22 are selected to reduce the number of samples.

Using same inductance and capacitance of all the antennas, the other parameters like coil antenna length, diameter, and resistance are calculated using equations (1-7). The ratio of length to diameter of coil antenna is called form factor. There are three groups of studies, two on helical antenna and one on spiral antenna. The two studies on helical antenna are carried on the variation of form factor i.e. on the variation of ratio of length to diameter of coil antenna. There are two critical form factor dimensions, diameter and length. Length-to-diameter ratio is important for two reasons [25-32]:

- Shorter lengths and larger diameters increase capacitance across the inductor. Capacitance across any inductor carrying time-varying current increases circulating currents in the inductor, increasing loss while simultaneously reducing system bandwidth.
- Longer lengths and smaller coil diameters reduce mutual coupling between turns and increase leakage flux. This results in use of increased conductor length for a given inductance, increasing wire resistance.

These two situations are obviously in direct conflict, a balance must be achieved. Optimum balance between conflicting L/D effects listed above depend heavily on external circuit capacitance and operating frequency. Hence for study, two types of form factor are chosen. The study can be summarized as:

1. Helical antenna 1 ($0.5 \leq \text{Form Factor} \leq 0.6$)
2. Helical antenna 2 ($1 \leq \text{Form Factor} \leq 1.65$)
3. Spiral Antenna

The parameters of helical antenna 1, helical antenna 2 are calculated using single-layer air coil equation (6). The parameters of spiral antenna are calculated using multi-layer air coil equation (7). The resistances are calculated using calcoil software. When length of the multilayer coil is kept equal to diameter of wire and increasing the single turn per layer, a spiral antenna is forms.

The maximum efficiencies for AWG 18 and AWG 14 wire are calculated using equations (11-13). The simulation result of maximum efficiency of wireless power transfer link using AWG 14, 18 and 22 wire for helical antenna is shown in figure 17.

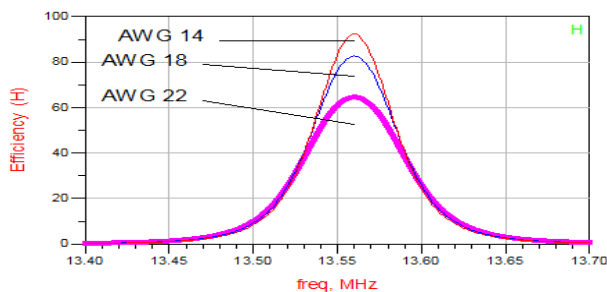


Figure 17: Power transfer efficiency of different wire gauge

The maximum efficiencies for AWG 18 and AWG 14 wire are calculated. The simulation result of maximum efficiency of wireless power transfer link using AWG 14, 18 and 22 wire for helical antenna is shown in figure 18.

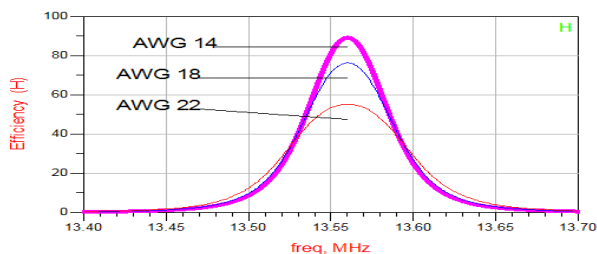


Figure 18: Power transfer efficiency of different wire gauge

The maximum efficiencies for AWG 18 and AWG 14 wire are calculated. The simulation result of maximum efficiency of wireless power transfer link using AWG 14, 18 and 22 wire for helical antenna is shown in figure 19.

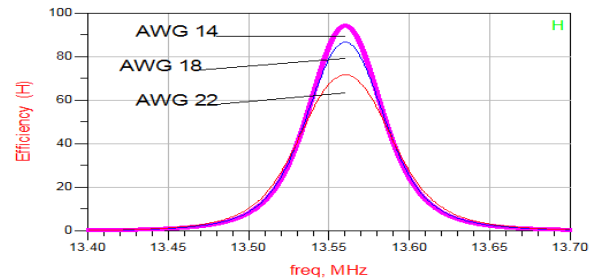


Figure 19: Power transfer efficiency of different wire gauge

The efficiency result for both calculated and simulated is summarized in the tables 6, 7 and 8 given below.

Table 6: Efficiency comparison of helical antenna1 at varying wire gauge

Helical antenna ($0.5 \leq \text{Form Factor} \leq 0.6$)		
Wire Gauge	Efficiency (%)	
	Calculated	Simulation
AWG 22	64.64	64.6
AWG 18	82.81	82.67
AWG 14	92.35	92.34

Table 7: Efficiency comparison of helical antenna2 at varying wire gauge

Helical antenna ($1 \leq \text{Form Factor} \leq 1.65$)		
Wire Gauge	Efficiency (%)	
	Calculated	Simulation
AWG 22	55.2	55.13
AWG 18	76.39	76.3
AWG 14	89.3	89.13

Table 8: Efficiency comparison of spiral antenna at varying wire gauge

Spiral antenna		
Wire Gauge	Efficiency (%)	
	Calculated	Simulation
AWG 22	71.74	71.58
AWG 18	86.86	86.56
AWG 14	94.3	94.15

7. Conclusion

In this paper, EPC1010 transistor, a GaN HEMT technology in a class-E amplifier, is used as shown in figure 7. Simulation results as shown in figure 8 show that due to its low on-state resistance and high-speed switching performance, it is very suitable for high frequency power amplifier of wireless power transfer system. Due to smaller size and low power consumption of GaN HEMT, it is most suitable for the wireless power system used in biological implants.

Also, for the power amplifier, class-E is a better choice as it is a low voltage high power high efficiency amplifier. From figure 4.3, it is clearly seen that a 5-volt dc drain input voltage causes sinusoidal output of amplitude 160 volts at 13.56 MHz.

It is seen from figure 11 when the distance between transmitter and receiver changes, the coupling coefficient (k) also varies and the resonant frequency (13.56MHz) splits. It can be seen from figure 12 that decreasing the coupling coefficient k_{23} between transmitter & receiver coils i.e. bringing the transmitter and receiver closer keeping the k_{12} & k_{34} fixed, efficiency of the system decreases and frequency splitting takes place. When the coupling between power coil and transmitter coil k_{12} is increased (keeping k_{23} & k_{34} fixed) from 0.1 to 0.2 i.e. bringing the power coil and transmitter coil closer, the frequency splitting phenomenon is eliminated and the efficiency of the system increases.

It can be seen from figure 13 that decreasing the coupling coefficient k_{23} between transmitter & receiver coil i.e. bringing the transmitter and receiver closer keeping the k_{12} & k_{34} fixed, efficiency of the system decreases and frequency splitting takes place. When the coupling between receiver coil and load coil k_{34} increase (keeping k_{12} & k_{23} fixed) from 0.1 to 0.25 i.e. bringing the receiver coil and load coil closer eliminates the frequency splitting phenomenon and the efficiency of the system increases.

From the simulation, it is found that reducing the source's internal resistance, and increasing the mutual inductance of the Power coil and the Transmitter coil, along with the mutual inductance of the receiver coil and the load coil, helps relieve the frequency splitting phenomena and improve efficiency.

In this work, two antenna topologies namely series-series as shown in figure 9 and mixed topology as shown in figure 14 are simulated and compared. In figure 15 and 16, the efficiency variation of the system with varying coupling coefficient is shown. In series-series topology, a slight variation of 0.006 in coupling coefficient causes the system efficiency to drop to 15 % and also frequency splitting takes place. On the other hand, mixed topology called LCC has shown better performance. The change of 0.025 in coupling coefficient of LCC topology only causes a change of 20% i.e. a decrease from 80% to 60% in the system efficiency. Hence, for minimizing the frequency, splitting the LCC topology is superior to the series-series topology.

Considering the types of wires, from table 6, 7 & 8, the efficiencies of Wireless Power Transfer using AWG 14, 18 and 22 wires of helical antenna 1 are shown. It is

seen that AWG 14 is greatly superior in efficiency as it has low resistance due to its cross-sectional area for all the antenna systems: helical antenna 1, helical antenna 2 and spiral antenna while AWG 22 has the least efficiency.

Considering the types of antenna, from table 6, 7 and 8, it is seen that efficiency of helical antenna 1 and spiral antenna is higher than efficiency of helical antenna 2 when AWG 22 is used. Also, the efficiencies of helical antenna 1 and spiral antenna are found to be almost same. When AWG 18 and AWG 14 are used, it is seen that the efficiency of spiral antenna is the best, while the efficiency of helical antenna 1 remains higher than that of helical antenna 2.

Comparing helical antenna 1 and helical antenna 2, these two antennas are different in form factor which is the measure of ratio of length to diameter of the antenna. If the form factor is less, then the antenna will be smaller and compact. As a result, such antenna tends to have better efficiency and also compact size. Hence, helical antenna 1 is the more suitable of the two.

While comparing helical antenna 1 and spiral antenna, we observe that the efficiency performance of spiral antenna is better for all wire types, AWG 14, 18 and 22. Also, spiral antenna is more compact than helical antenna and can be fabricated easily in Integrated Circuits (ICs), the applications where size and efficiency are main constraints, as in biological implants, where spiral antenna is the best choice.

From the observations and analyses done so far in this paper, it can be concluded that the use of GaN HEMT class-E amplifier gives the best efficiency in the Wireless Power Transfer Link with AWG 14 wire, spiral antenna and LCC topology.

References

- [1] W. Chen, R. A. Chinga, S. Yoshida, J. Lin, C. Chen, and W. Lo, "A 25.6 W 13.56 MHz wireless power transfer system with a 94% efficiency GaN class-E power amplifier," *Microwave Symposium Digest (MTT)*, 2012 IEEE MTT-S International, pp. 1-3, August 2012.
- [2] William C. Brown, "The history of wireless power transmission," *Solar Energy*, vol.56, no.1, pp. 3-21, Jan. 1996
- [3] Kurs, A. Karalis, R. Moffatt, J. D. Joannopoulos, P. Fisher and M. Sojajic, "Wireless Power Transfer via Strongly Coupled Magnetic Resonances," *Massachusetts Institute of Technology*, 2007 Science, Vol. 317. no. 5834, pp. 83-86, July 2007.
- [4] Zhang, Xiu, S. L. Ho, and W. N. Fu. "Analysis and Optimization of Magnetically Coupled Resonators for Wireless Power Transfer," *IEEE Transactions on Magnetics*, vol. 48, no.11, pp.4511-4514, November 2012.

- [5] Chen, Linhui, Shuo Liu, Yong Chun Zhou, and Tie Jun Cui, "An optimizable circuit structure for high-efficiency wireless power transfer," *IEEE Transactions on Industrial Electronics*, vol. 60, no. 1, pp.339-349, January 2013.
- [6] Nadakuduti, Jagadish, Lin Lu, and Paul Guckian, "Operating frequency selection for loosely coupled wireless power transfer systems with respect to RF emissions and RF exposure requirements," *In Wireless Power Transfer (WPT)*, 2013 IEEE, pp. 234-237. IEEE, May 2013.
- [7] Karalis, Aristeidis, John D. Joannopoulos, and Marin Soljačić. "Efficient wireless non-radiative mid-range energy transfer." *Annals of Physics* 323.1, pp. 34-48, January 2008
- [8] Babic, Slobodan I., Frederic Sirois, and Cevdet Akyel. "Validity check of mutual inductance formulas for circular filaments with lateral and angular misalignments." *Progress In Electromagnetics Research M*, vol. 8, pp. 15-26, 2009
- [9] Grover, Frederick W. "The calculation of the mutual inductance of circular filaments in any desired positions." *Proceedings of the IRE* 32.10, pp. 620-629, 1944
- [10] Lundin, Richard. "A handbook formula for the inductance of a single-layer circular coil." *Proceedings of the IEEE* 73.9, pp. 1428-9, 1985
- [11] Grover, Frederick W. *Inductance calculations: working formulas and tables*. Courier Dover Publications, 2004.
- [12] http://en.wikipedia.org/wiki/American_wire_gauge
- [13] Nilsson, James William., and Susan A. Riedel. *Electric Circuits*. Boston: Prentice Hall, 2011. Print
- [14] Kawamura, Atsuo, and Tae-Woong Kim. "Proposed Equivalent Circuit and Parameter Identification Method for Electro-Magnetic Resonance Based Wireless Power Transfer." April 2013
- [15] Beh, TeckChuan, et al. "Wireless Power Transfer System via Magnetic Resonant Coupling at Fixed Resonance Frequency—Power Transfer System Based on Impedance Matching—." *Proc. The 25th World Battery, Hybrid and Fuel Cell Electric Vehicle Symposium & Exhibition (EVS25)*. November 2010.
- [16] Sokal, Nathan O. "Class-E RF power amplifiers." *QEX Commun. Quart* 204, pp. 9-20, 2001
- [17] de Rooij, Michael A., and Johan T. Strydom. "eGaN FETs in Low Power Wireless Energy Converters." *ECS Transactions* 50.3, pp. 377-388, 2013
- [18] Uchiyama, Hiroyuki, et al. "Consideration of impact of GaN HEMT for class E amplifier." *TENCON 2010-2010 IEEE Region 10 Conference*. IEEE, 2010.
- [19] http://epc-co.com/epc/documents/datasheets/EPC1010_datasheet.pdf
- [20] Sah, Ajay Kumar and Timalsina, Arun. "Design of Simple Wireless Power Transfer System via Magnetic Resonant Coupling at 13.56MHz." *Proceedings of IOE Graduate Conference*, Vol. 1, pp. 206-210, November 2013
- [21] Yang, Ching-Wen, and Chin-Lung Yang. "Analysis on numbers and adaptive ranges of resonators for efficient resonant coupling wireless power transmission." *Wireless Power Transfer Conference (WPTC), 2014 IEEE*. IEEE, 2014.
- [22] Zhang, Y., Zhengming Zhao, and Kainan Chen. "Frequency Splitting Analysis of Four-Coil Resonant Wireless Power Transfer.", *Energy Conversion Congress and Exposition (ECCE)*, 2013 IEEE , pp. 1-1, September 2013
- [23] Yiming Zhang, Zhengming Zhao and Kainan Chen, "Frequency splitting analysis of magnetically-coupled resonant wireless power transfer," *Energy Conversion Congress and Exposition (ECCE)*, 2013 IEEE , pp.2227-2232, 15-19 September 2013.
- [24] Y. Zhang, Z. Zhao and K. Chen, "Frequency decrease analysis of resonant wireless power transfer," *IEEE Trans. Power Electron.*, vol. 29, no. 3, pp. 1058-1063, Mar. 2014.
- [25] Waters, Benjamin H., et al. "Optimal coil size ratios for wireless power transfer applications." *Circuits and Systems (ISCAS), 2014 IEEE International Symposium on*. IEEE, 2014.
- [26] Yan, Zhuo, et al. "Influence Factors Analysis and Improvement Method on Efficiency of Wireless Power Transfer Via Coupled Magnetic Resonance." *Magnetics, IEEE Transactions on* 50.4, pp. 1-4, 2014
- [27] Choi, Hyo-Jin, Sangbin Lee, and Cheolung Cha. "Optimization of geometric parameters for circular loop antenna in magnetic coupled wireless power transfer." *Wireless Power Transfer Conference (WPTC), 2014 IEEE*. IEEE, 2014.
- [28] Sample, Alanson P., David A. Meyer, and Joshua R. Smith. "Analysis, experimental results, and range adaptation of magnetically coupled resonators for wireless power transfer," *IEEE Transactions on Industrial Electronics*, vol. 58, no. 2, pp. 544-554, February 2011.
- [29] Hwang, Hyeonseok, et al. "An analysis of magnetic resonance coupling effects on wireless power transfer by coil inductance and placement." *Consumer Electronics, IEEE Transactions on* 60.2, pp. 203-209, 2014
- [30] Fu, Minfan, et al. "Subsystem-level efficiency analysis of a wireless power transfer system." *Wireless Power Transfer Conference (WPTC), 2014 IEEE*. IEEE, 2014.
- [31] Zhang, Yiming, Zhengming Zhao, and Ting Lu. "Quantitative Analysis of System Efficiency and Output Power of Four-Coil Resonant Wireless Power Transfer." *IEEE Transactions on Power Electronics*, pp. 1-1, 2013.
- [32] Pozar, David M. *Microwave engineering*. John Wiley & Sons, 2009.
- [33] Jordan, Edward C., and K. G. Balmain. *Electromagnetic Waves and Radiating Systems*. Second ed. New Dehli: Prentice-Hall of India, 2006. Print.
- [34] Jonah, Olutola, "Optimization of Wireless Power Transfer via Magnetic Resonance in Different Media," Ph.D. Thesis, FIU Electronic Theses and Dissertations, Paper 876, March 2013.